Universiteit Utrecht

University Utrecht

Bachelor Thesis

Natuur en Sterrenkunde

Reconstruction of the Σ_c-baryon using the ALICE detector

Author:
Sebastiaan van Duinen
Student number:
3707768

Supervisor:
Dr. Alessandro Grelli
Co-Supervisor:
Msc. Syaefudin Jaelani

June 12, 2019

Abstract

At the end of 2017 an ALICE collaboration paper was published in which they measured a Λ_c^+/D^0 production ratio that is 5 times higher than the expected value measured by other experiments. The only difference being that the recent measurement was done in pp and p-pB collisions. A potential explanation for this deviation is that the overproduction of Λ_c^+ is a direct result of an increased Σ_c production within the pp and p-pB collisions as Σ_c decays into Λ_c^+ and $\pi^\pm$ 100% of the time. Due to the low halftime of the Σ_c-baryon, no distinction can be made between the Λ_c^+ from the Σ_c and prompt Λ_c^+'s originating from a charm quark. In order to gain more information regarding the properties of the Σ_c-baryon, a reconstruction of the Σ_c is attempted. This is done using Pythia8 to simulate the production of Σ_c and looking at its decay into Λ_c^+ and $\pi^\pm$. In particular the angle of decay between the two daughter particles is studied and used to find and apply cuts in the ALICE-dataset which consists of experimental data from pp collisions at $\sqrt{s} = 6.5$ TeV. The reconstruction resulted in the observation of Σ_c^{++} and the observation of Σ_c^0 both in the p_T range of [12-16] GeV/c. Studying the angle of decay proved to be feasible in the reconstruction of the Σ_c-baryon in high p_T ranges, but further research is required in order to confirm its discovery.

Contents

1 Introduction

An ALICE collaboration paper was published at the end of 2017 [1] in which they calculated the production ratio of the Λ_c^+/D_0 from the datasets of the pp and p-Pb collisions at $\sqrt{s} = 7$ TeV and $\sqrt{S_{NN}} = 5.02$ TeV respectively. These results were compared with the expectation values obtained from perturbative Quantum Chromodynamics calculations and Monte Carlo event generators. The measured Baryon-to-meson ratio for pp collisions is

$$\left(\frac{\Lambda_c^+}{\mathrm{D}^0}_{pp}\right) = 0.543 \pm 0.061(\text{stat.}) \pm 0.160(\text{syst.}),$$

and that for the p-Pb equation is

$$\left(\frac{\Lambda_c^+}{\mathrm{D}^0}_{p-Pb}\right) = 0.602 \pm 0.060(\text{stat.})^{+0.159}_{-0.087}(\text{syst.}).$$

As can be seen in Table 1 which reports the measurements in e^+e^- and ep collisions, the measured ratios are significantly higher compared to the expected values.

	$\Lambda_c^+/D^0 \pm$ stat. $\pm$ syst.	System	$\sqrt{s}$(GeV)	Notes
CLEO [43]	$0.119 \pm 0.021 \pm 0.019$	ee	10.55	
ARGUS[42,98]	0.127 ± 0.031	ee	10.55	
LEP average [80]	$0.113 \pm 0.013 \pm 0.006$	ee	91.2	
ZEUS DIS [51]	$0.124 \pm 0.034^{+0.025}_{-0.022}$	ep	320	$1 < Q^2 < 1000GeV^2$, $0 < p_T 10GeV/c, 0.02 < y < 0.7$
ZEUS γp HERA I [49]	$0.220 \pm 0.035^{+0.027}_{-0.037}$	ep	320	$130 < W < 300GeV, Q^2 < 1GeV^2$, $p_T > 300GeV, Q^2 < 1GeV^2$
ZEUS γp HERA II [50]	$0.107 \pm 0.018^{+0.009}_{-0.014}$	ep	320	$130 < W < 300GeV, Q^2 < 1GeV^2$, $p_T > 3.8GeV/c \lvert\eta\rvert < 1.6$

Table 1: Comparison of the Λ_c^+/D^0 ratio as measured in e^+e^- collision systems and at different centre-of-mass energies as published in the ALICE collaboration paper [1]

One of the reasons why this finding is interesting is that this deviation from the expected values indicates that the fragmentation of heavy-flavour baryons is not yet well understood. A potential explanation for this deviation in the measured ratios of Λ_c^+/D^0 could be due to a change in the production rate of the Σ_c-baryons in pp and p-Pb collisions as opposed to ee and ep collision systems. The mean lifetime of a Σ_c-baryon is around $(2.97 \pm 1) \cdot 10^{-22}$ s[2], so it has long been decayed before reaching a detector. The decay of Σ_c to $\Lambda_c^+ + \pi$ is 100% and because of the short lifetime of the Σ_c, the Λ_c coming from the Σ_c cannot be distinguished from the prompt Λ_c's originating directly from a charm quark by the detectors. In addition in Pb-Pb collisions we expect to create the so called Quark-Gluon Plasma (QGP). The QGP is a plasma phase of matter where quarks and gluons are not anymore bounded in hadrons

but are free to move. Cosmological models predict that all the matter of our Universe was in a QGP phase a few microseconds after the Big Bang. Therefor having the possibility to investigate the plasma would be of major interest for multiple branches of physics. In particular the possibility to investigate the Σ_c production in Pb-Pb collisions and to compare it with the production in pp collisions would allow us to understand if the plasma modifies the charm hadronization mechanism.

This thesis will be focused around attempting to reconstruct the Σ_c allowing more clarity regarding the measured deviation between the fragmentation ratios which could provide answers as to whether universality is broken or not and potentially provide more information regarding quark-gluon plasma. This reconstruction will be attempted by looking at the angle of decay of the Σ_c-baryon into Λ_c^+ and $\pi^{\pm}$. which leads to the following research question:

Is it possible to reconstruct the Σ_c-baryon by applying cuts from the angle of decay of the Σ_c-baryon with the ALICE detector at the LHC in Cern?

2 Theory

2.1 Alice

ALICE is a detector within the Large Hardron Collider that is designed to detect subatomic particles in order to study physics of strongly interacting matter at extreme densities.[3] The ALICE detector consists of 19 sub-detectors but not all are relevant for this thesis. The sub-detectors relevant for this thesis are the Inner Tracking System, the Time Projection Chamber, the Time Of Flight detector and the High Momentum Particle Identification Detector. The Alice operator can detect particles with a transverse momentum ranging between 100 MeV/c to 100 GeV/c [4]

2.1.1 Inner Tracking System

The Inner Tracking System (ITS) consists of 6 layers of silicon detectors that covers a pseudo-rapidity range of $|\eta| \leq 0.9$. These 6 layers of slides are separated into 3 groups. The first two layers are made of Silicon Pixel Detectors, the two middle layers are made of Silicon Drift Detectors and the two outermost layers are made of double sided Silicon Strip Detectors. The Silicon Drift Detectors The ITS is used to determine the primary and secondary vertices (points where particles are produced via the collision of beam particles, via the decay of particles or via interaction with the detector) [5] which are necessary for the reconstruction of charm decays. The ITS also identifies and tracks low momentum particles and improves the momentum and angle measurements of the TPC [6]

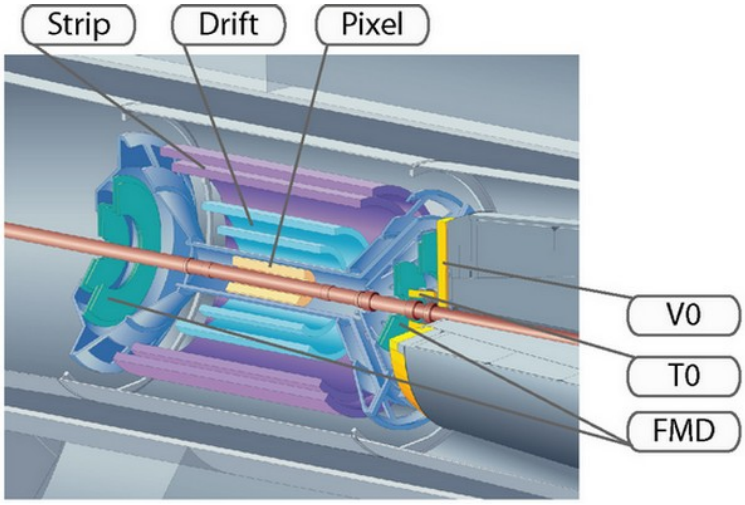

Figure 1: A computer generated image showing the Inner Tracking System and where the different Silicon Detectors are positioned.[7]

2.1.2 Time Projection Chamber

The Time Projection Chamber (TPC) is a large cylindrical volume filled with gas. Charged particles traversing through the TPC ionize the gas. The resulting electrons drift due to an electric field towards the end plates of the cylinder. There are 557.568 pads that read these

signals resulting in 3-D information of the trajectory of the particles and measurement of the energy loss of the particles. This energy loss can be used to identify particles. TPC's are known to produce lots of information but when it comes to tens of thousands of charged particles this provides a guaranteed way of reliable information.[6] The TPC also has a pseudorapidity range of $|\eta| \leq 0.9$ and can measure p_{T} values of up to 100 GeV [4]

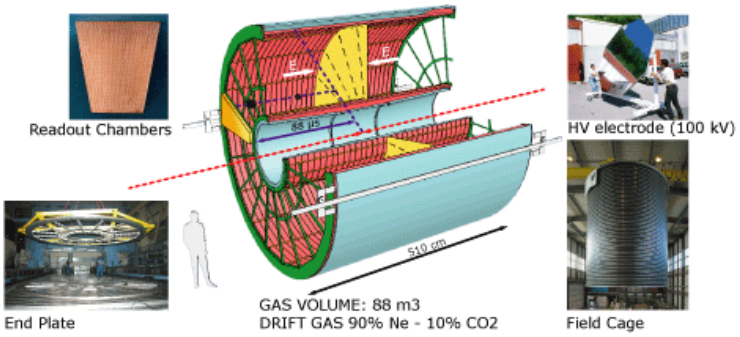

Figure 2: Schematic view of the Time Projection Chamber [8]

2.1.3 Time Of Flight

The Time of Flight detector (TOF) has the purpose of identifying charged particles up to 2.5 GeV/c [9] which covers a pseudorapidity range of $|\eta| \leq 0.9$ [10]. It does so by measuring the flight time of particles from the collision over a given distance along the track trajectory. If the momentum of the particle is identified as well, the mass of the particles can be derived. The TOF detector is a large area array of multigap resistive plate chambers containing a total of 1593 detector elements that cover a cylindrical surface of 141 m^2

2.1.4 High Momentum Particle Identification Detector

For charged particles with a momentum too large for the TOF ITS and the TPC to detect there is the High Momentum Particle Identification Detector (HMPID). The HMPID is a Ring imaging Cherenkov detector which is made up of two parts, a radiator medium where the Cherenkov light is produced and a photon detector to generate images of the Cherenkov light. If a particle traverses through a medium faster than light would in that medium, photons are emitted under a characteristic angle based on the velocity of the particle. The photon detector measures these characteristic angles providing information regarding the velocity of the particles.[11]

2.2 Standard Model

The standard model is currently the best theory describing subatomic physics.[12] It describes the interaction between subatomic particles that are governed by the fundamental forces. Currently the standard model successfully describes and explains three of the four

fundamental forces with only gravity being a problem. The standard model includes three families of particles. Leptons, which have no strong interaction, Quarks which make up all hadrons and Gauge Bosons which are particles that mediate interactions. There are 6 different types of leptons: electron, muon, tau and their respective neutrino. There are also 6 different types of quarks: up, down, charm, strange, top and bottom. For the gauge bosons there are the gluons, which mediate the strong interaction among quarks, photons that mediate the electromagnetic interaction and the $W^{\pm}$ and Z^0 particles that mediate the weak interaction. As such it is proposed that the hypothetical graviton should mediate the gravitational interaction. [12] These particles form the fundamental building blocks of matter. Particles that are made up of 3 quarks or 3 anti-quarks are called baryons, such as protons and neutrons which have up up down and up down down quarks respectively. Particles that are made up of 2 quarks (a combination of a quark with an anti-quark) are called fermions, such as pions and kaons.

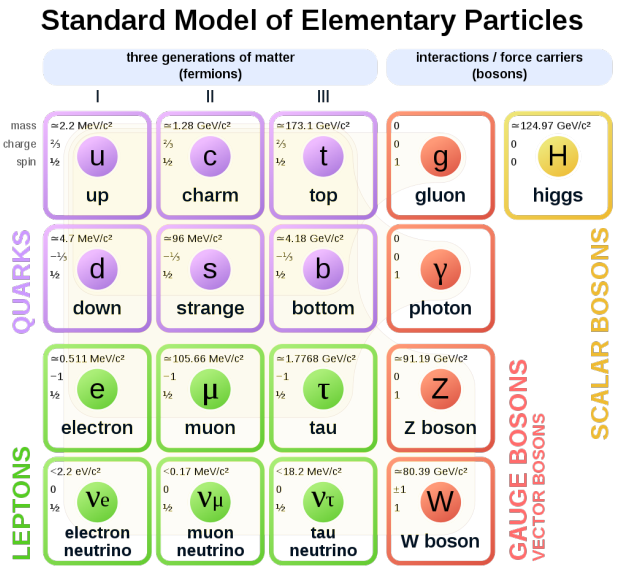

Figure 3: This is the commonly used figure[13] to showcase the core concepts of the standard model. As mentioned, there are 6 quarks, 6 leptons, the gauge bosons and since recently there is also a scalar boson, the higgs boson. All of these also have their respective anti-particle which has similar mass but opposite charge and other subatomic quantities such as strangeness, lepton number, etc.

2.3 Relevant definitions

I will discuss some definitions and equations that are necessary to understand the thesis.

2.3.1 Transverse momentum

The transverse momentum is the component of the momentum that is perpendicular to the beam line. The reason this is important is because the momentum parallel to the beam line may be left over from the beam particles. The transverse momentum is related to what

happened at the vertex. As such, if we take the axis parallel to the beam line to be the z-axis, the transverse momentum is given by

$$p_t = \sqrt{p_x^2 + p_y^2} \tag{1}$$

2.3.2 Pseudo-rapidity

A definition I already mentioned previously, the pseudorapidity η is the spatial coordinate which describes the angle of a particle with respect to the beam axis and is defined as

$$\eta \equiv -\ln\left[\tan\left(\frac{\theta}{2}\right)\right] \tag{2}$$

with θ being the angle between the three-momentum $\mathbf{p}$ and the direction of the beam axis.

2.3.3 Invariant mass and Center of Mass energy

After a particle decays into other particles, the energy and momentum of the other particles can be used to determine the mass of the parent particle. The mass is invariant meaning that it is independent of the reference frame in which the energy and momenta were measured. The energy-momentum relationship is given by

$$\mathrm{E}^2 = (pc^2)^2 + (m_0^2c^2)^2,$$

which, given the conservation of energy and momentum, can be rewritten to

$$m_0 = \sqrt{\left(\frac{\mathrm{E}_1 + \mathrm{E}_2}{c^2}\right)^2 - \left(\frac{p_1 + p_2}{c}\right)^2}, \tag{3}$$

with E_1, p_1, E_2 and p_2 the energy and momentum of the two tracks and m_0 the invariant mass of the parent particle.

The center of mass energy ($\sqrt{s}$) is the energy of the particles colliding into each other from the reference frame of the center of mass from the two particles. This is given by

$$\sqrt{s} = \sqrt{p^\mu p_\mu} = \sqrt{E^2/c^2 - \vec{\mathbf{p}}}. \tag{4}$$

Here, $\vec{\mathbf{p}}^\mu$ is the four-momentum with E/c as first component and the three-momentum as the second to fourth components. The minkowski norm squared of the four-momentum gives the center of mass energy with E the energy of the particle, c the speed of light and $\vec{\mathbf{p}}$ the three-momentum given by $\vec{\mathbf{p}} = (p_x, p_y, p_z)$.
If two particles with masses m_1 and m_2 collide, the total center of mass energy can be

calculated as follows

$$\begin{aligned}\sqrt{s} &= \sqrt{(p_1^\mu + p_2^\mu)^2} \\ &= \sqrt{\frac{(E_1+E_2)^2}{c^2} - (\vec{\mathbf{p}}_1 + \vec{\mathbf{p}}_2)^2} \\ &= \sqrt{p_1^2 + m_1^2c^2 + p_2^2 + m_2^2c^2 + \frac{E_1E_2}{c^2} - p_1^2 - p_2^2 - \vec{\mathbf{p}}_1 \cdot \vec{\mathbf{p}}_2} \\ \sqrt{s} &= \sqrt{m_1^2c^2 + m_2^2c^2 + \frac{E_1E_2}{c^2} - p_1p_2\cos(\theta)} \end{aligned} \tag{5}$$

2.3.4 Significance

The significance is a very important quantity in particle physics. It quantifies whether a finding is significant enough to be considered an observation or even a discovery. Collisions result in large amounts of data. In order to reconstruct a particle, simulations are done to cut away large chunks of data. Afterwards, a fit is applied on the remaining data. The fit is made up of two equations, one being a Gaussian function which should follow the peak of the signal if a signal is present and one to fit the background data. These equations provide values for the parameters used for the fit which can be used to gain information regarding the signal. In order to calculate the significance of the signal, the mean and the standard deviation of the signal are integrated over the range of $[\mu - 3\sigma, \mu + 3\sigma]$. Then, combined with the integral of the background over the same range, the significance α is given by

$$\alpha = \frac{S}{\sqrt{S+B}} \tag{6}$$

Because the fit of the signal is Gaussian, the Gaussian statistics can be applied to tell what values of α are required for it to be an observation or a discovery. If this value of α is higher than 3, the finding is considered to be an observation. So the particle is most likely there, but it requires further research in order to conclusively call it a discovery. If the value of α is higher than 5, the finding is considered to be a discovery. The data analysis is accurate enough to conclusively show the existence of that particle.

2.4 Particle information

For the reconstruction of the Σ_c, it's important to understand properties regarding its decay into Λ_c^+ and $\pi^\pm$

2.4.1 The Σ_c-baryon

There are three different Σ_c-baryons: Σ_c^{++}, Σ_c^+ and Σ_c^0 with their respective antiparticles. The Σ_c-baryon has only one decay channel.

$$\begin{aligned} \Sigma_c^{++} &\to \Lambda_c^+\pi^+ \quad (100\%) \\ \Sigma_c^{+} &\to \Lambda_c^+\pi^0 \quad (100\%) \\ \Sigma_c^{0} &\to \Lambda_c^+\pi^- \quad (100\%) \end{aligned} \tag{7}$$

With the mean halftime of Σ_c being around $(2.97 \pm 1) \cdot 10^{-22}$ seconds [1], the mean travel distance is given by $c\tau \approx 8.9 \cdot 10^{-14} m$. Given that the ITS can only detect secondary vertices separated by at least 100 μm from the primary vertex, the Σ_c-baryon has long decayed by the time it could be measured by the ITS detector. Since all Σ_c-baryons decay into Λ_c^+ and $\pi^\pm$, it is very much possible that the measured production rate of the Λ_c^+-baryon as described in the ALICE collaboration paper [1] measured both Λ_c^+-baryons coming from the Σ_c-baryon and prompt Λ_c^+-baryons. For this thesis I will only focus on the Σ_c^++-baryon and the Σ_c^0-baryon because the Σ_c^+-baryon decays into an electrically neutral pion which isn't picked up by the electric field in the ALICE detector. For the remainder of this thesis, whenever Σ_c is mentioned, both the Σ_c^{++}-baryon and Σ_c^0-baryon are referred to. Because the Σ_c-baryon can be in different quantum states, different masses can be measured. According to the Particle Database Group, the invariant masses of the Σ_c-baryon are as follows[14]

$$\begin{aligned} \Sigma_c(2455)^{++} &\rightarrow m = 2453.98 \pm 0.16 \text{MeV} \\ \Sigma_c(2455)^{0} &\rightarrow m = 2453.74 \pm 0.16 \text{MeV} \\ \Sigma_c(2520)^{++} &\rightarrow m = 2517.9 \pm 0.6 \text{MeV} \\ \Sigma_c(2520)^{0} &\rightarrow m = 2518.8 \pm 0.6 \text{MeV} \end{aligned} \tag{8}$$

2.4.2 The Λ_c^+-Baryon

The Λ_c^+-baryon has many different decay channels. The decay channel used for reconstruction is the decay of lambda into a p, K^- and π^+ .

$$\Lambda_c^+ \rightarrow \text{p}\text{K}^-\pi^+(5 \pm 1.3\%)[14] \tag{9}$$

Because the mean distance traveled by the Λ_c^+ is $c\tau = 59.9 \cdot 10^{-6}$ m [14], the Λ_c^+ is too short to be detected. Therefore, just like with the Σ_c-baryons, the Λ_c-baryons must be reconstructed from the properties of the daughter particles. In particular the proton, kaon and the pion from the decay mentioned above.

2.4.3 The $\pi^\pm$-meson

Because pions are among the most abundant type of meson, each pp collision results in lots of pions. Charged pions are easily detected because their halftime is much larger than that of the Λ_c^+ and the Σ_c. The halftime of a charged pion is around $(2.6 \pm 0.0005) \cdot 10^{-8}$ seconds [14] which means that the mean distance is then given by $ct \approx 7.795$ m. This lies within the range of the detectors and can therefore easily be measured. In order to distinguish between the pions resulting from the decay of the Σ_c and the prompt pions, the properties of the pions resulting from the decay of the Σ_c are studied. Both the transverse momentum of the pions and the angle of decay between the Λ_c^+-baryons and the pions are studied with the hopes of finding specific properties allowing a reduction of the background noise.

[1] The halftime of Σ_c is calculated by $\tau = \hbar/\Gamma$, with $\Gamma = 2.2 \pm 0.4$ MeV [14], $\hbar$ = planck's constant/2π and τ = the halftime.

3 Simulations and Results

In an attempt to reconstruct the Σ_c-baryon simulations have to be done in order to find specific information of the decay event and the daughter particles allowing for cuts in the dataset from ALICE. After the cuts have been applied,

3.1 Simulations

3.1.1 ROOT and Pythia

In order to obtain specific information regarding the particles involved in the decay of the Σ_c-baryon, a simulation of the pp collision. This simulation was done using a program, Pythia 8.210[15], for the generation of high-energy physics. Pythia 8 was run using ROOT 6.10/08[16], which is a data analysis framework that allows codes written in C++ and other languages such as Python and R. Root has newer versions available but due to continuous problems with installing these latest versions an older version was opted which worked. ROOT is specifically designed for particle physics data analysis, allowing for high computing efficiency. A pre-made basic collision event generator code is used as a basis on which the rest of the simulation is build.[17] Pythia 8 has build in codes allowing to force certain aspects of collision events. Since the focus of this thesis is to investigate charmed particles, a force was applied in the simulation such that the pp collisions would produce more charm/anti-charm quarks. This reduces the simulation time by huge margins because charmed quarks have a low production rate. This forcing was done as instructed on the Pythia 8 website.[18] The code used is added in the appendix A.1

3.1.2 Cuts

Given that the pseudorapidity range of the ALICE detectors is given by $|\eta| < 0.9$, a cut on the $|\eta|$ has been placed, preventing the simulation of particles with η values outside of this range. The collision energy is set at $\sqrt{s} = 6.5$ TeV[19]. For each Σ_c particle generated, the p_{T} is requested. In order to obtain specific information regarding the decay particles of the Σ_c-baryon, selections were made based on the values for the p_{T} of the Σ_c. The p_{T} value ranges simulated are [0-1,1-2, 2-3, 3-4, 4-6, 6-12, 12-16, 16-24] GeV/c. Based on the p_{T} ranges of the Σ_c, all daughter particles are separated in order to obtain specific information. On top of that, the angle of decay is calculated based on the momentum of the Λ_c^+ and the π, also based on the p_{T} ranges of the Σ_c. Using a tree construction all this data is saved so that after a large simulation, the data of each individual quantity can be read whenever necessary. The angle of decay values from the Σ_c are compared to a background distribution of θ^*. Dividing the simulated angle of decay from the Σ_c by the background distribution the specific angles with which the Σ_c decays into Λ_c^+ and $\pi^{\pm}$ becomes clear. Based on the range of these angles, cuts can be applied on the dataset from ALICE to cut away irrelevant particles.
So the applied cuts are the η cut with $|\eta| < 0.9$, the specific p_{T} ranges for the $\pi^{\pm}$ as obtained from the simulations per p_{T} range of the Σ_c and the specific angles of decay per p_{T} range of the Σ_c.

3.1.3 Invariant mass fits

After the cuts found by the simulation runs are applied on the dataset of ALICE, the reconstruction of the Σ_c is attempted. The resulting mass plots are fitted via two equations. A second degree polynomial function was used for the background and a Gaussian function for the signal. If the fit shows a peak around the expected value for the invariant mass it could mean that, depending on whether the significance is a value larger than 3 or 5, the reconstruction of the Σ_c is successful. If the significance turns out to be less than 3, more cuts should be applied or the current cuts should be done more precisely.

3.2 Results

3.2.1 Simulations and cut ranges

The simulation has run over 50 million charm-forced pp collisions at $\sqrt{s} = 6.5$ TeV. Since one of the decay products of the Σ_c is the $\pi^{\pm}$ and due to it having p_{T} values of less than 100 MeV in the ranges [0-1, 1-2] GeV/c, they have been cut out. The following ranges will be studied: [2-3, 3-4, 4-6, 6-12, 12-16]. The simulation lasted for 44 hours and after applying the η cut, 17.898 Σ_c^{++}- and 17.977 Σ_c^0-baryons were found, however a large part resides in the 0-1 and 1-2 GeV/c p_{T} range which have been cut out, showing that even after forcing charm/anti-charm quarks, Σ_c-baryons are difficult to generate. The normalized pion distribution based on the $\Sigma_c p_t$ ranges can be seen in figure 4 and 5. A very important note is that the error bars in the higher p_{T} ranges are not representative of the actual error margin. Due to the way the simulated events were written into the tree construction, whenever a Σ_c particle was found it would write an extra unchanged value for all the p_{T} ranges that were outside of the p_{T} range of the detected particle. As a result, especially for higher p_{T} ranges where fewer particles were found, the same value was assigned many times over resulting in an increased accuracy of measurement in the plots reducing the size of the error bars. Since the only purpose of these plots was to find the range within which the $\pi^{\pm}$ were produced in order to find the p_{T} values at which to cut in the ALICE dataset, this isn't an issue. As a result of these plots, the p_{T} values that were selected to cut in the p_{T} range of the pions are shown in table 2

p_{T} **ranges of the** Σ_c **in GeV/c**	p_{T} **cut ranges for** π^+ **in GeV/c**	p_{T} **cut ranges for** π^- **in GeV/c**
[2,3]	[0,0.35]	[0,0.35]
[3,4]	[0,0.5]	[0,0.46]
[4,6]	[0.1,0.7]	[0.1,0.65]
[6,12]	[0.12,1.2]	[0.2,1.15]
[12,16]	[0.5,1.5]	[0.4,1.5]

Table 2: Cut ranges based on the p_{T} ranges of the Σ_c parent particle. The π^+ comes from the Σ_c^{++} and the π^- comes from the Σ_c^0

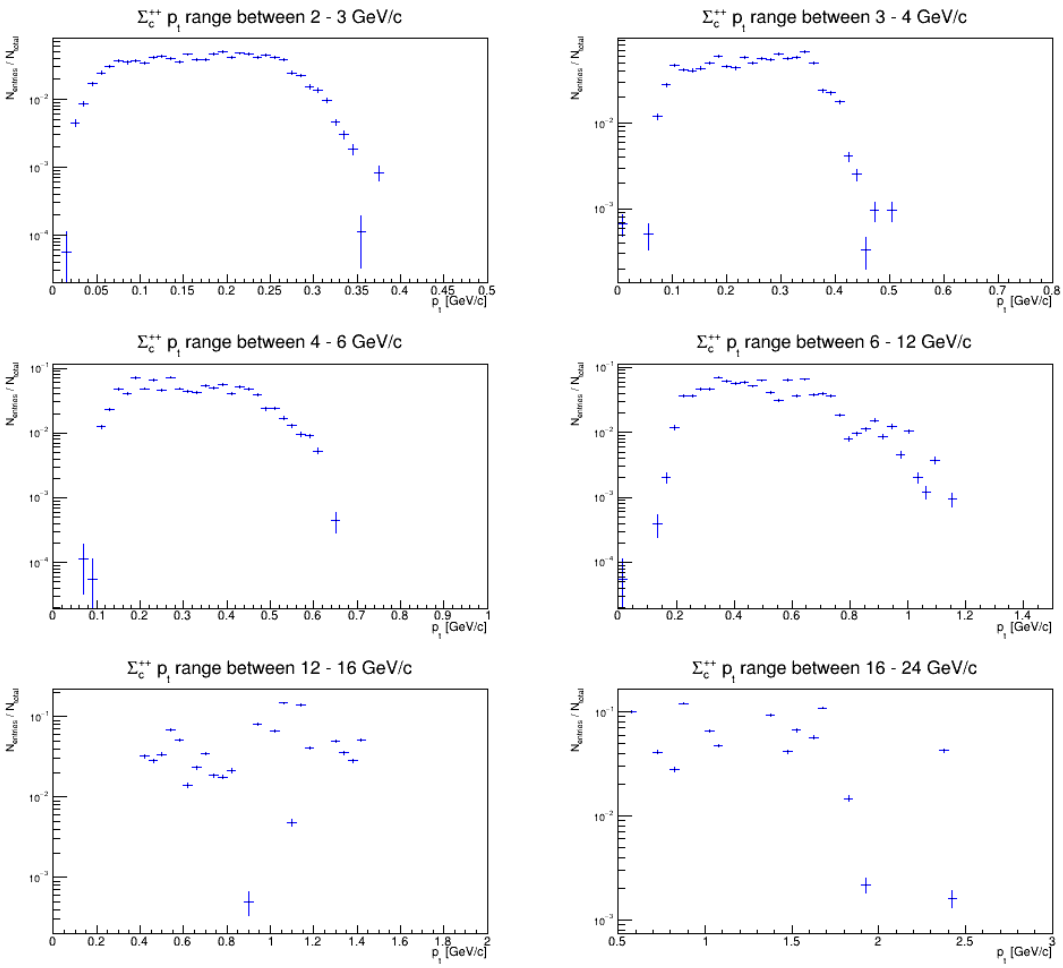

Figure 4: Normalized p_{T} distribution of the π^+ per p_{T} range of Σ_c^{++} with on the y-axis the entries divided by the total data points in order to normalize the histogram and on the x-axis the p_{T} range in GeV/c. The y-axis has been set as a logarithmic axis in order to quickly spot where the particles stop appearing.

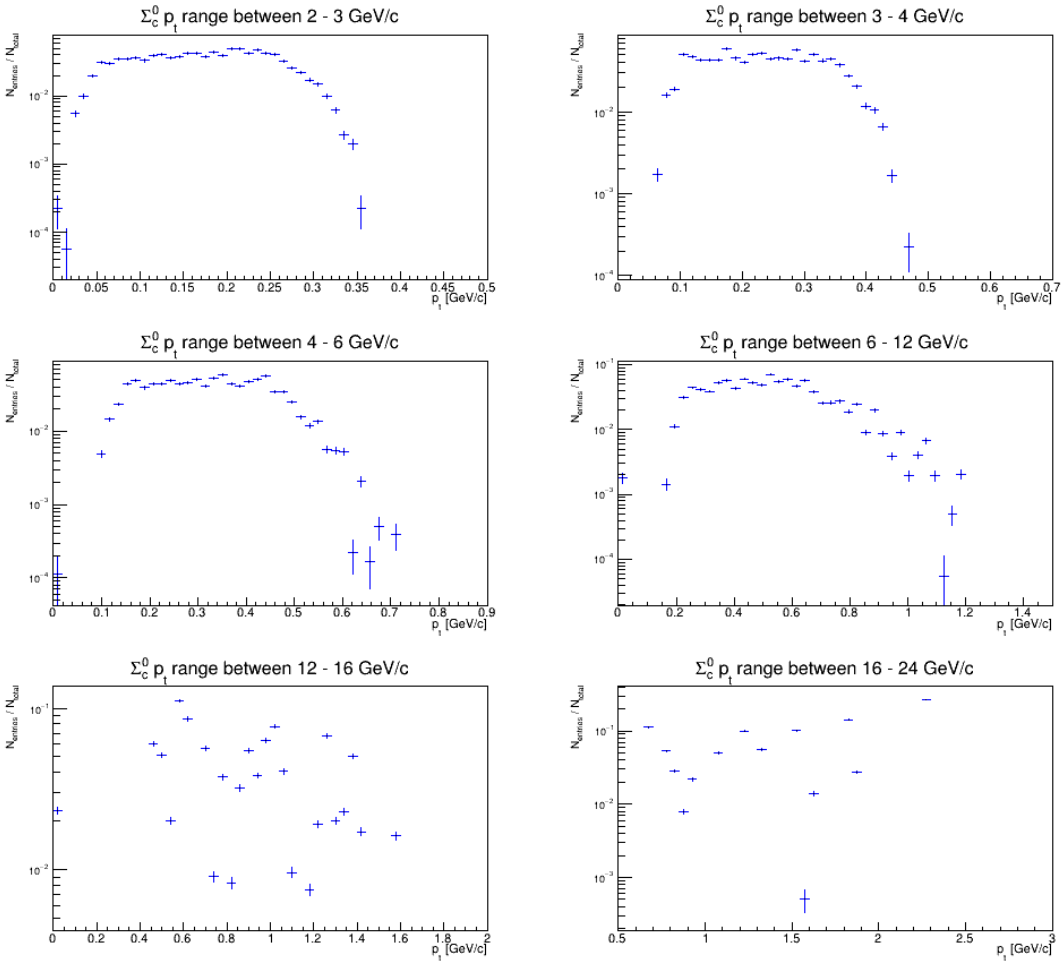

Figure 5: Normalized p_{T} distribution of the π^- per p_{T} range of Σ_c^0 with on the y-axis the entries divided by the total data points in order to normalize the histogram and on the x-axis the p_{T} range in GeV/c. The y-axis has been set as a logarithmic axis in order to quickly spot where the particles stop appearing.

The third cut that is applied is the cut based on the specific angle of decay of the Σ_c-baryon. In figures 6 and 7 you can see the comparison of cos(θ) distribution from the Σ_c and the cos(θ) distribution from the θ* from the ALICE dataset. For the sake of clarity I have zoomed in to the relevant area in order to show the shape of the angle of decay distribution of the Σ_c. In the Appendix A.1 the unzoomed plots can be seen in order to get a better grasp of how much background signal was cut via the comparison between the two distributions. The angle of decay distribution of the Σ_c-baryon is shifted further to the right which suggests that the $\pi^{\pm}$ and the Λ_c^+ are closer together due to the angle of decay being small . Especially in the higher p_{T} ranges, [4-6,6-12,12-16,16-24], this shift seems to be strong.

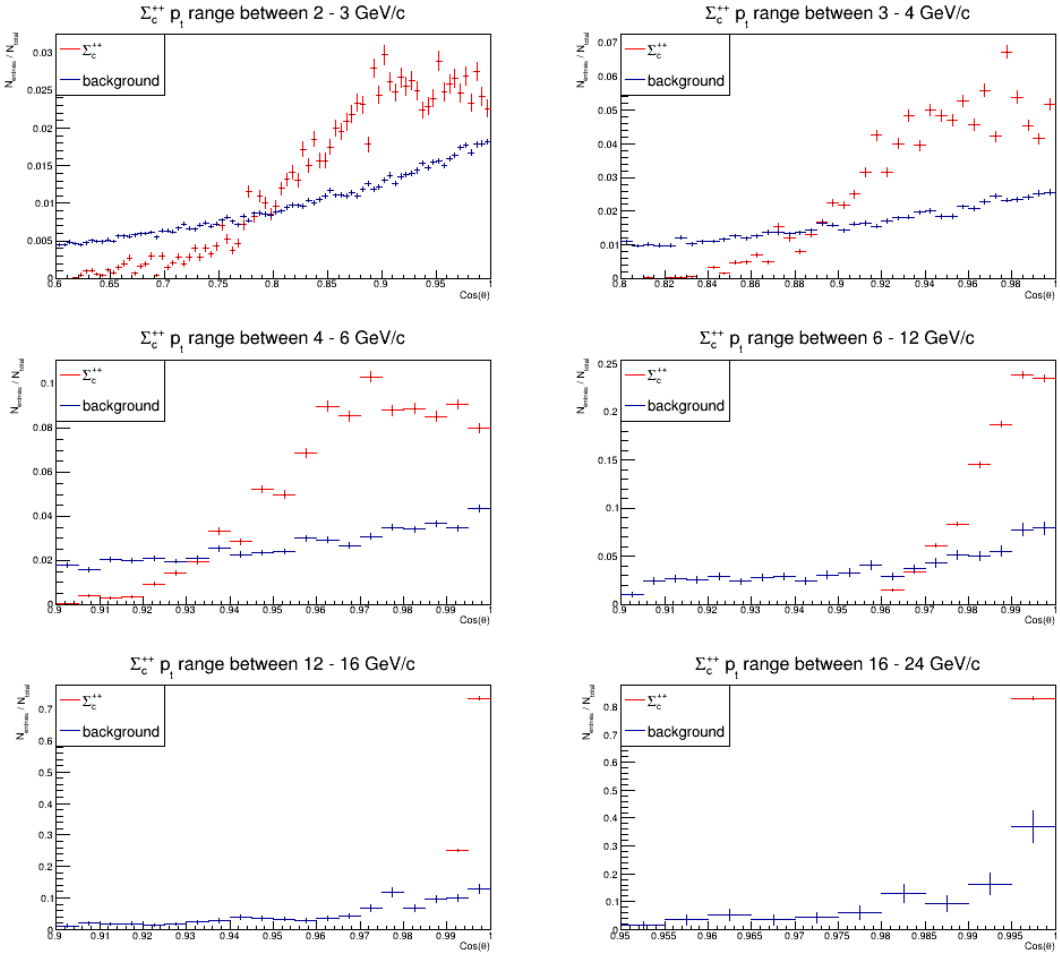

Figure 6: Normalized distribution from the cos(θ) of the decay of Σ_c^{++} compared to the cos(θ) of the θ^*, with on the y-axis the entries divided by the total data points in order to normalize the histogram and on the x-axis the angle in terms of cos(θ).

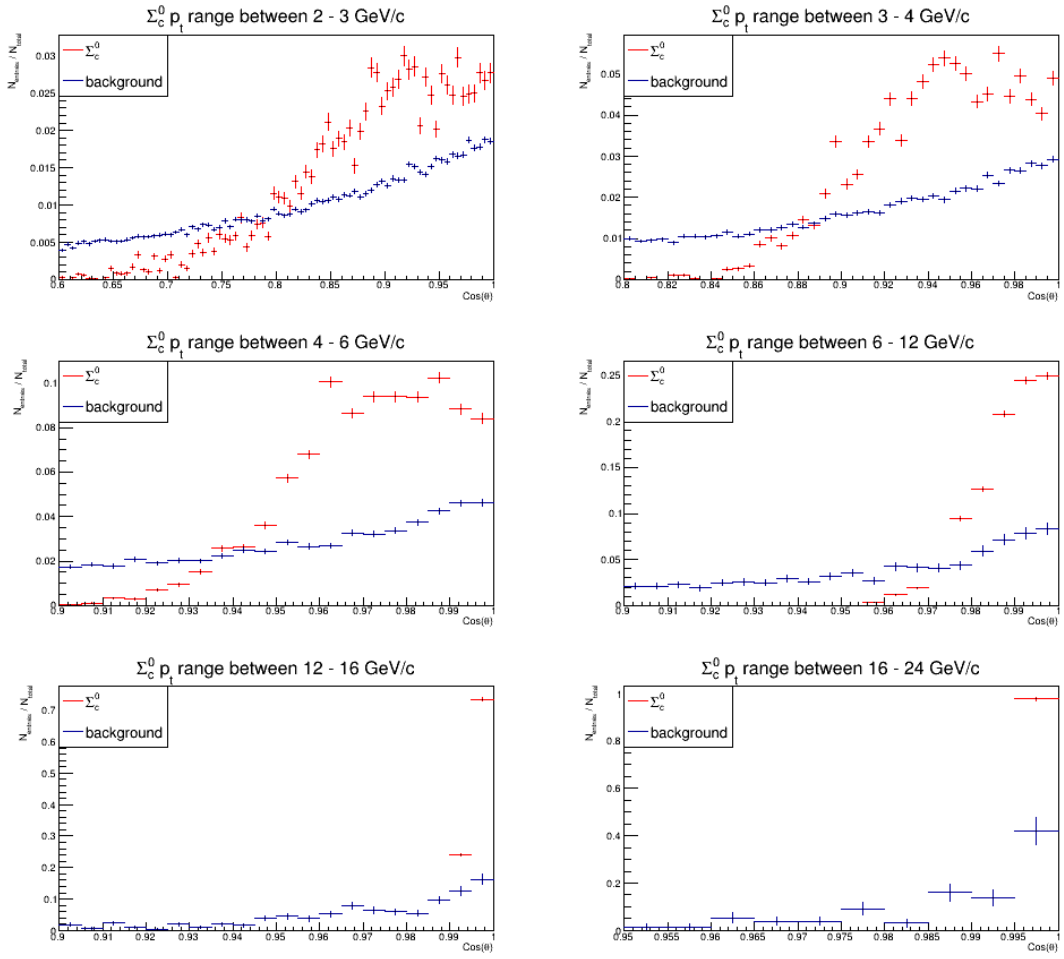

Figure 7: Normalized distribution from the cos(θ) of the decay of Σ_c^{++} compared to the cos(θ∗) of the θ^*, with on the y-axis the entries divided by the total data points in order to normalize the histogram and on the x-axis the angle in terms of cos(θ)

In order to get a better idea on where exactly to cut, ratio plots were made by dividing the entries of the angle of decay distribution of the Σ_c by the entries of the θ^* distribution. As a result, entries above the value of 1 will indicate where the Σ_c distribution provides more entries than the θ^* distribution. The ratio plots 8 and 9 Give a clear view on where the cuts should be applied. These plots show that for every p_{T} range significant cuts can be made. As mentioned before, especially the high p_{T} ranges provide good clear cuts in the background with up to 6 times more entries in the p_{T} range of [12-16] GeV/c.
Based on ratio plots 8 and 9 cuts were made which are presented in table 3 As expected, the higher p_{T} ranges provide really good cuts, allowing to cut away the majority of the background while maintaining most of the signal.

Σ_c^{++}	p_t range (GeV/c)	Cuts made at (cos(θ))	Signal remaining (%)	Bg removed (%)
	2-3	0.78-1	89.9	44.2
	3-4	0.89-1	90.2	56.4
	4-6	0.94-1	94.1	62.8
	6-12	0.9725-1	98.5	64.2
	12-16	0.992-1	93.5	77.0
Σ_c^{0}	p_t range (GeV/c)	Cuts made at (cos(θ))	Signal remaining (%)	Bg removed (%)
	2-3	0.78-1	89.3	43.7
	3-4	0.88-1	93.8	50.9
	4-6	0.945-1	90.6	62.3
	6-12	0.9725-1	98.7	62.3
	12-16	0.992-1	100	71.2

Table 3: The applied cuts in the ALICE-dataset based on the ratio plots. The percentage of remaining signal and background have been calculated by integrating over the remaining entries within the range left over after the cuts have been applied. Since the plots have been normalized the value after integration multiplied by 100% gives the percentage of the remaining signal or background.

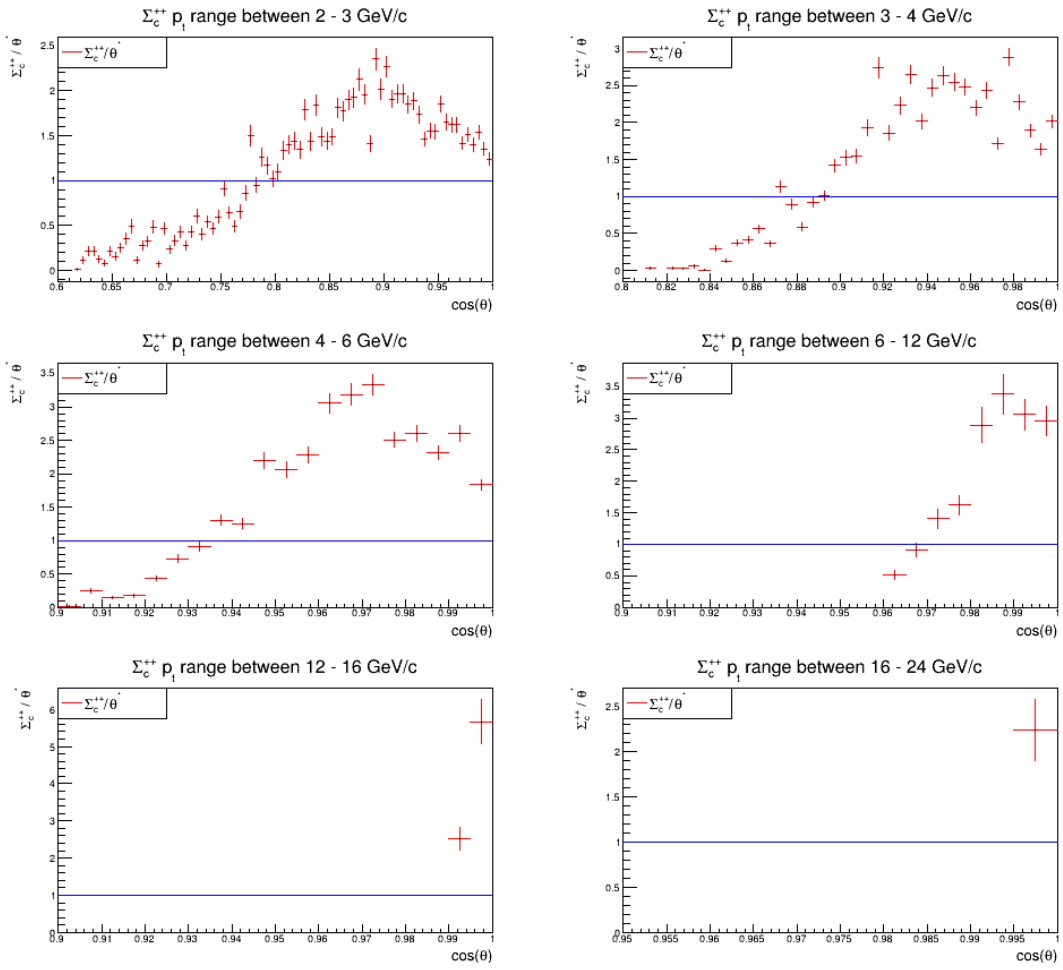

Figure 8: The ratio plots between the angle of decay distribution of Σ_c^{++} against the θ^* distribution per p_{T} range of Σ_c^{++}

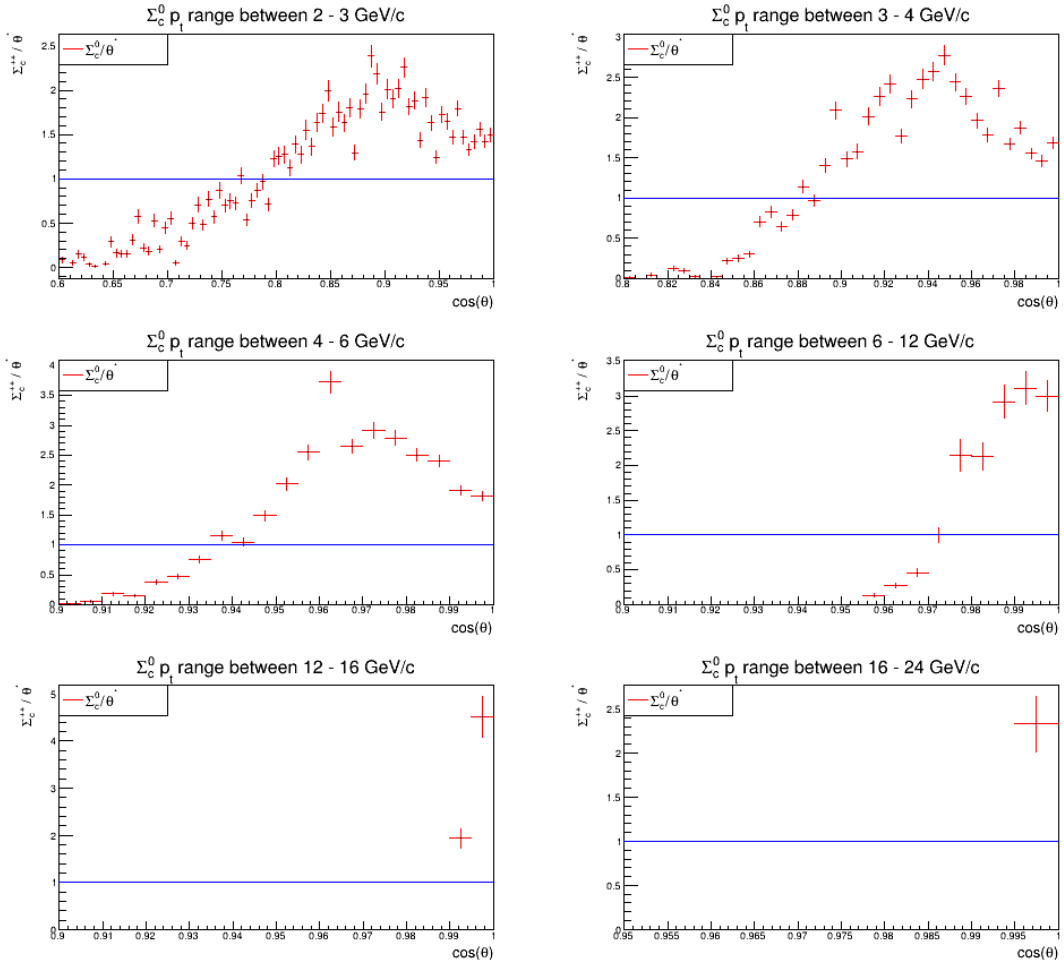

Figure 9: The ratio plots between the angle of decay distribution of Σ_c^0 against the θ^* distribution per p_{T} range of Σ_c^0

3.2.2 Invariant mass distributions, fit and significance

The cuts found in table 3 have been applied to the ALICE-dataset. From the remaining particles, Λ_c^+ and $\pi^\pm$ are reconstructed and based on that, the Σ_c is reconstructed. The invariant mass is calculated using equation 3 from section 2.3.3. After the invariant mass has been calculated, the difference in the invariant masses of the Σ_c's and the Λ_c^+'s are calculated which results in the invariant mass distribution as shown in figures 10 and 11

based on the theoretical value for the invariant mass of $\pi^\pm$ [14], the peak is to be expected at
$\delta m_{\pi^+} = m_{\Sigma_c^{++}} - m_{\Lambda_c^+} = 167.56 \pm 0.11$ MeV for the Σ_c^{++}, and
$\delta m_{\pi^-} = m_{\Sigma_c^0} - m_{\Lambda_c^+} = 167.30 \pm 0.11$ MeV for the Σ_c^0

As can be seen in figures 10 and 11, there are far more entries in the lower p_T ranges [2-3, 3-4, 4-6] GeV/c than in the higher p_T ranges [6-12, 12-16, 16-24] GeV/c. This makes finding a reliable signal less likely in the higher p_T ranges where the cuts based on the simulations were most effective.

Looking at figure 10, A small signal can be seen around the expected value of $\delta m_{\pi^+} \approx 167$ MeV for the p_T ranges of [4-6, 6-12]. A larger signal can be seen in the p_T ranges of [12-16, 16-24] GeV/c. As expected, nothing can be seen in the lower p_T ranges of [2-3, 3-4] GeV/c. A small bump can consistently been seen around $145 MeV/c^2$ in the first three plots. The fits have been applied and seem to follow the the datapoints properly. A gaussian peak appears in the five plots with p_T range of [3-4, 4-6, 6-12, 12-16, 16-24] GeV/c respectively, however the peak in the p_T range of [3-4] GeV/c seems to be too low. As a result of the successful fits, the integral over the signal fit over the range of $\mu \pm 3\sigma$ was calculated, as well as the integral of the background fit over the same range. Using those two values, the significance was calculated as described in section 2.3.4 equation 6. The resulting values can be found in table 4.

Looking at figure 11, again a small signal appears around the expected value of $\delta m_{\pi^-} \approx 167$ MeV for the p_T ranges of [3-4, 4-6, 12-16, 16-24] GeV/c of the Σ_c^0-baryon. Nothing can be seen in the lowest p_T range of [2-3] GeV/c. The p_T range of [6-12] GeV/c stands out because it seems to have a dip at the expected value of $m_{\pi^-} = 167.30 \pm 0.11$ MeV. The last plot in the p_T range of [16-24] GeV/c shows well how low amounts of entries result in strongly varying data and thus provides unreliable information. Again, the fits have been applied and seem to follow the the datapoints properly. A gaussian peak appears in all of the six plots, although it's barely visible in the first two plots. As a result, the integral over the signal fit over the range of $\mu \pm 3\sigma$ was calculated, as well as the integral of the background fit over the same range. Using those two values, the significance was calculated as described in section 2.3.4 equation 6. The resulting values can be found in table 4.

What's interesting to notice is the appearance of a peak around the mass of 145MeV/c^2 in multiple plots for varying ranges. $145 MeV/c^2$ is the mass of the soft pion with low momentum. It could be that during the reconstruction of the invariant mass due to potentially

improper application of the cuts, some soft pions remained but due to the deadline of this thesis there is not enough time left to investigate this further.

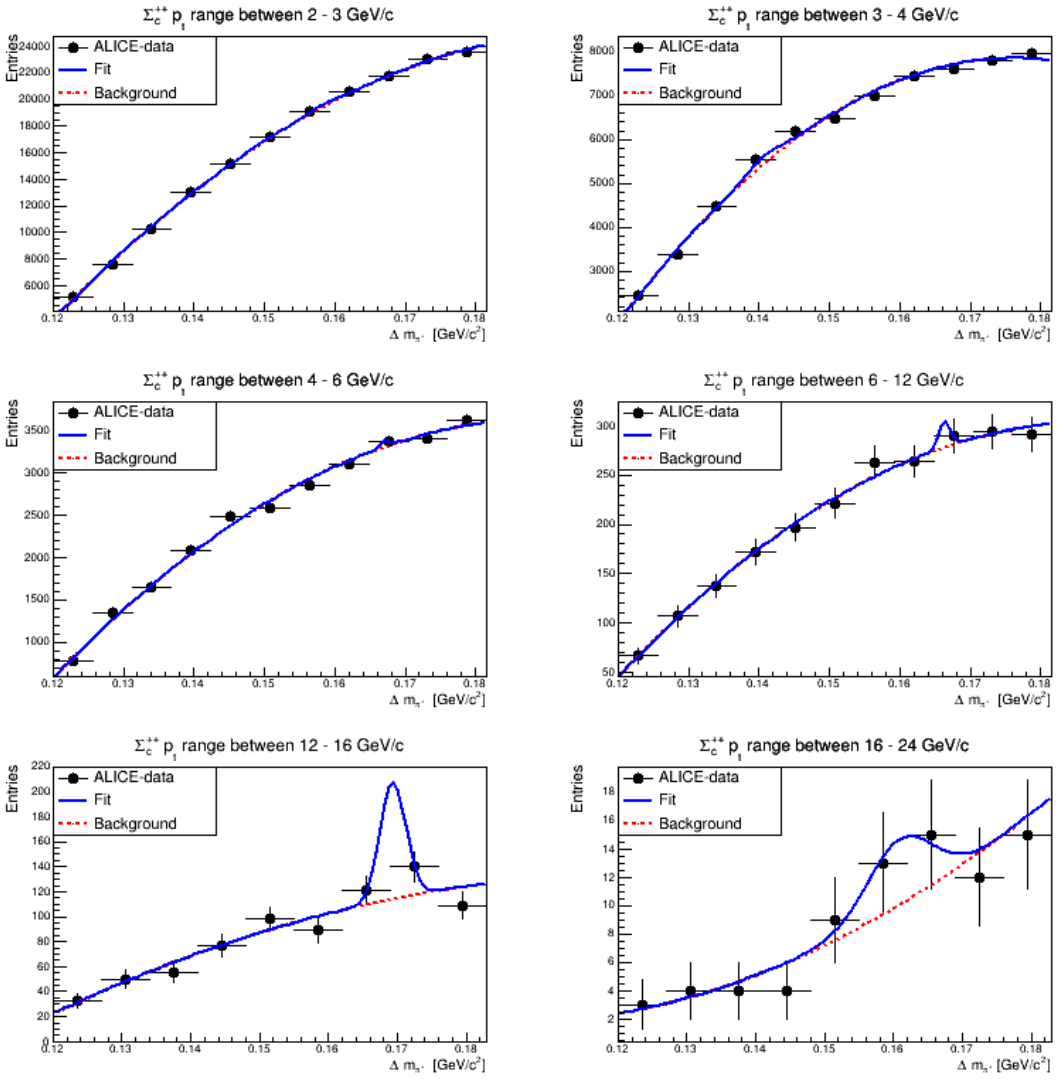

Figure 10: The fitted invariant mass plots of the reconstructed $\Sigma_c^{++} - \Lambda_c^+$ per p_{T} range as a result of applied cuts from the simulations.

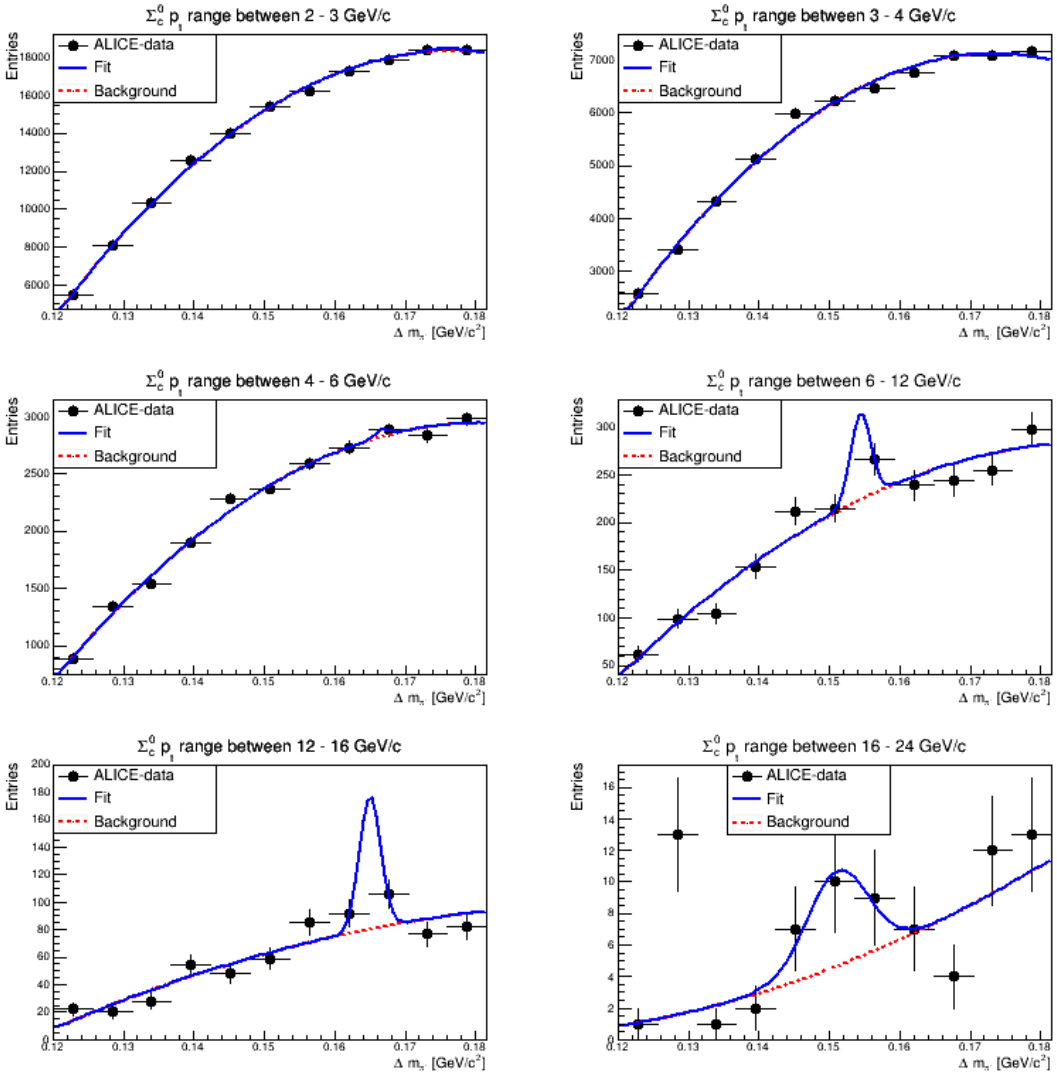

Figure 11: The fitted invariant mass plots of the reconstructed $\Sigma_c^0 - \Lambda_c^+$ per p_{T} range as a result of applied cuts from the simulations.

When looking at table 4 it can be seen that for both Σ_c-baryons, the reconstruction was successful enough in the p_{T} ranges of [12-16] as they both have a significance value that is larger than 3. Based on the definition of the significance, it could be concluded that the Σ_c has thus been observed. However when looking at the plots, it seems that due to the low amount of entries enough fluctuations occur resulting in unreliable information. The Σ_c^0-baryon also shows a peak with a relatively high significance in the p_{T} range of [6-12]. However this peak has its mean value at $154\mathrm{MeV}/c^2$. All the other significance values are too low to be considered an observation. However, it is important to note that the mean of the gaussian peak for the Σ_c^0 at a p_{T} range of [12-16], ($\delta \mathrm{m}_{\pi^-} = 164.99 \pm 1.524$ MeV), is not within the error margin of the expected value, ($\delta \mathrm{m}_{\pi^-} = 167 \pm 0.11$ MeV). This is probably due to a fluctuation of the datapoints, forcing the mean to be a bit further to the left, which results in a lower measured value of the $\delta \mathrm{m}_{\pi^-}$.

Σ_c^{++}	$p_{\mathbf{T}}$ **range (GeV/c)**	**Mean mass of signal (MeV)**	**Standard deviation**	**Significance** (α)
	2 - 3	158.184	2.652	0.45
	3 - 4	140.925	2.391	0.94
	4 - 6	167.121	0.658	0.51
	6 - 12	166.372	0.843	0.64
	12 - 16	169.345	1.869	3.15
	16 - 24	160.918	4.741	0.55
Σ_c^0	$p_{\mathbf{T}}$ **range (GeV/c)**	**Mean mass of signal (MeV)**	**Standard deviation (MeV)**	**Significance** (α)
	2 - 3	175.762	2.542	0.46
	3 - 4	166.995	1.004	0.09
	4 - 6	166.741	0.983	0.48
	6 - 12	154.406	1.474	2.32
	12 - 16	164.990	1.524	3.67
	16 - 24	151.185	4.362	0.85

Table 4: The mean value of the signal, the standard deviation and the corresponding significance of the signal found in the invariant mass plots of the Σ_c reconstruction based on the applied cuts from the simulations.

4 Conclusions

Looking back at the simulations in table 3 they seem effective. Lots of background is removed with hardly any loss of signal. This leads to conclude that the angle of decay of the Σ_c is definitely a viable option to use as a cut for the reconstruction of Σ_c. However since most of the cutting happens in the higher p_{T} ranges, [4-6, 6-12, 12-16, 16-24], this method is mainly useful as a high-p_{T} cut.

Looking at the invariant mass plots and the fits, only significant peaks can be seen in the p_{T} ranges of [4-6, 6-12, 12-16], excluding the Σ_c^0 p_t range of [6-12] which has a signal but at the wrong mass. Especially in the p_{T} range of [4-6] GeV/c, the signals can be seen clearly, however small they may be. Both the 145 MeV and the 167 MeV bumps indicate the detection of a pion and they appear for both Σ_c^{++} and Σ_c^0. Given the amount of entries and as a result the little amount of fluctuations in the ALICE-data points, this provides a good indicator that the angle of decay cuts are effective.

After having calculated the significance for all the p_{T} ranges, the observation of the Σ_c-baryon was made in the p_{T} range of [12-16] GeV/c for both Σ_c^0 and Σ_c^{++} with a significance of 3.15 and 3.67 respectively. No discovery was made as none of the values for the calculated significance exceeded the value of 5.

Aside from the $\Sigma_c(2445)$, the $\Sigma_c(2520)$ was subject to reconstruction. However, no sign of a peak could be found at the invariant mass of 231 MeV/c^2 (which is the invariant mass of the $\pi^{\pm}$ as a result of the decay of $\Sigma_c(2520)$) and was therefor left out of this thesis.

It is also important to note that the Σ_c^{++} and the Σ_c^0 react equally well on the angle of decay cut.

Because there are simply not enough Σ_c entries at high p_{T} range, the random fluctuations are large enough to make any observation difficult for p_{T} ranges higher than 6 GeV/c. Since the angle of decay cut is mainly effective at this range, this proves to be quite a limitation.

Based on these results, the reconstruction of the Σ_c using the angle of decay to cut background noise proves to be possible, but due to its limitations it is recommended to apply different cuts that focus more on the low-momentum Σ_c-baryons. Further research into different cutting-methods will most likely result in a proper reconstruction of the Σ_c-baryon which could help answer questions regarding the measured fragmentation ratio of the Λ_c/D^0 from the ALICE collaboration paper[1]. On top of that, a proper reconstruction of the Σ_c could also help us understand if the plasma modifies the charm hadronization mechanism

5 Discussion

As mentioned in the conclusions 4, further research can be done regarding the reconstruction of the Σ_c-baryon. This could be done by investigating the decay of the Λ_c^+-baryon into

$pK^-\pi^+$. This was briefly attempted for this thesis but due to an unknown problem regarding the simulation of the daughter particles, was left out of this thesis. Studying this decay could provide useful information regarding the Σ_c as it provides more information regarding the pions, which could help cut away background data in the lower p_{T} ranges. The cuts resulting from the daughter particles of the Λ_c combined with the angle of decay cuts and the pion cuts from the Σ_c, could prove to be effective enough to reconstruct a Σ_c-baryon, as the Σ_c-baryon was already observed for the higher p_{T} ranges in this thesis.

Another thing that could be improved for further attempts at the reconstruction of the Σ_c-baryon is by making the Pythia8 simulations more realistic by implementing uncertainty based on the resolution of the detectors. This way the simulation more realistically mimics the data as measured by the ALICE-detectors which provides more accurate comparisons, which should result in better cuts.

Having that said, attempting to optimize the angle of decay cuts seems to be unwise as other options are still feasible. The limitations of the angle of decay cuts make the cuts really effective in ranges where there are hardly any data-points. Unless ALICE gets an upgrade, allowing for either a bigger data-set or higher momentum pp collisions, this cut would only work well in combination with other cuts.

Further research could also be done regarding the $\pi^{\pm}$ from the Σ_c decay, improving on the basic cuts that were applied. However the basic cuts that were applied didn't show any sign of cutting enough background to even see a hint of the π at the expected values in the lower p_{T} ranges. So this might be feasible but the other options were mentioned above seem more plausible as my results show no sign of the cuts being effective.

6 References

References

[1] ALICE collaboration et al. λ c+ production in pp collisions at$\sqrt{}$ s= 7 tev and in p-pb collisions at$\sqrt{}$ snn= 5.02 tev. *Journal of High Energy Physics*, 2018(4):108, 2018.

[2] ALICE. *Heavy ions and quark-gluon plasma*, Accessed: 08-06-2019. https://home.cern/science/physics/heavy-ions-and-quark-gluon-plasma.

[3] ALICE. *ALICE*, Accessed: 08-06-2019. https://home.cern/science/experiments/alice.

[4] Christian Lippmann. Performance of the alice time projection chamber. *Physics Procedia*, 37:434–441, 2012.

[5] Are Strandlie and Rudolf Frühwirth. Track and vertex reconstruction: From classical to adaptive methods. *Reviews of Modern Physics*, 82(2):1419, 2010.

[6] C Fabjan and J Schukraft. The story of alice: Building the dedicated heavy ion detector at lhc. *arXiv preprint arXiv:1101.1257*, 2011.

[7] ALICE. *The present Inner Tracking System - Steps forward!*, Accessed: 08-06-2019. http://alicematters.web.cern.ch/?q=ALICE_currentITS.

[8] ALICE. *The ALICE Time Projection Chamber (TPC)*, Accessed: 09-06-2019. http://aliceinfo.cern.ch/Public/en/Chapter2/Chap2_TPC.html.

[9] G Dellacasa, X Zhu, M Wahn, FM Staley, V Danielian, TL Karavicheva, DP Mikhalev, N Carrer, M Gheata, G Stefanek, et al. Alice technical design report of the time-of-flight system (tof). Technical report, 2000.

[10] Jaroslav Adam, Dagmar Adamová, Madan M Aggarwal, G Aglieri Rinella, Michelangelo Agnello, Nikita Agrawal, Zubayer Ahammed, Shafqat Ahmad, Sang Un Ahn, S Aiola, et al. Determination of the event collision time with the alice detector at the lhc. *The European Physical Journal Plus*, 132(2):99, 2017.

[11] Alejandro García Ernest M Henley. *Subatomic Physics*. World Scientific Publishing Co. Pte. Ltd, July 13, 2007. Page 68.

[12] Roger A. Freedman Hugh D. Young. *University Physics*. Pearson Education, inc., 2008. Pages 1522,1523,1525-1531.

[13] Wikipedia. *Standard Model of Elementary Particles*, accessed:12-06-2019. https://en.wikipedia.org/wiki/Gauge_boson#/media/File:Standard_Model_of_Elementary_Particles.svg.

[14] Claude Amsler, M Doser, M Antonelli, DM Asner, KS Babu, H Baer, HR Band, RM Barnett, E Bergren, J Beringer, et al. *Review of particle physics*, 2008. http://pdg.ge.infn.it/2008/tables/rpp2008-sum-baryons.pdf, pages (33,37,38).

[15] torbjorn. *Homepage*, accessed:12-06-2019. http://home.thep.lu.se/~torbjorn/Pythia.html.

[16] CERN. *Download release 6.10/08*, accessed:12-06-2019. https://root.cern.ch/content/release-61008.

[17] CERN. *Pythia8.C*, accessed:12-06-2019. https://root.cern.ch/root/html/tutorials/pythia/pythia8.C.html.

[18] torbjorn. *QCD Processes*, accessed:12-06-2019. http://home.thep.lu.se/~torbjorn/pythia81html/QCDProcesses.html.

[19] Cian O'Luanaigh. First successful beam at record energy of 6.5 tev. 2015.

A Appendix

A.1 Code used to force the charm/anti-charm quark production

```
// Configure
   pythia8->ReadString("HardQCD:hardccbar = on");
   pythia8->ReadString("HardQCD:gg2ccbar = on");
   pythia8->ReadString("HardQCD:qqbar2ccbar = on");
```

A.2 The full code for the generation of the particles and writing them in a tree construct

```
#include "TROOT.h"
#include "TSystem.h"
#include "TH1F.h"
#include "TClonesArray.h"
#include "TPythia8.h"
#include "TParticle.h"
#include "TDatabasePDG.h"
#include "TCanvas.h"
#include "TTree.h"
#include "TFile.h"



void fivemil(Int_t nev  = 50000000 , Int_t ndeb = 1)
{
   const char *p8dataenv = gSystem->Getenv("PYTHIA8DATA");
   if (!p8dataenv) {
      const char *p8env = gSystem->Getenv("PYTHIA8");
      if (!p8env) {
         Error("pythia8.C",
               "Environment variable PYTHIA8 must contain path to pythia
   directory!");
         return;
      }
      TString p8d = p8env;
      p8d += "/xmldoc";
      gSystem->Setenv("PYTHIA8DATA", p8d);
   }
   const char* path = gSystem->ExpandPathName("$PYTHIA8DATA");
   if (gSystem->AccessPathName(path)) {
         Error("pythia8.C",
               "Environment variable PYTHIA8DATA must contain path to $PYTHIA8
   /xmldoc directory !");
      return;
   }
// Load libraries
#ifndef G__WIN32 // Pythia8 is a static library on Windows
   if (gSystem->Getenv("PYTHIA8")) {
      gSystem->Load("$PYTHIA8/lib/libpythia8");
   } else {
      gSystem->Load("libpythia8");
```

```
40    }
41 #endif
42    gSystem->Load("libEG");
43    gSystem->Load("libEGPythia8");
44
45
46
47 //ptranges
48 Int_t ptbins = 8;
49 Int_t xmin[8]={0,1,2,3,4,6,12,16};
50 Int_t xmax[8]={1,2,3,4,6,12,16,24};
51
52 // Two Trees + leaves
53         TFile *f1 = new TFile("50mil_1.root","recreate");
54         TTree *t1 = new TTree("t1","A tree for Sigmac++");
55 Float_t ptspp[ptbins],pts[ptbins],etaspp[ptbins], etas[ptbins];
56 Float_t ptsppl[ptbins],ptspppion[ptbins],ptspplpion[ptbins],ptspplkaon[ptbins
    ],ptspplproton[ptbins];
57 Float_t etasppl[ptbins],etaspppion[ptbins],etaspplpion[ptbins],etaspplkaon[
    ptbins],etaspplproton[ptbins];
58 Float_t ptsl[ptbins],ptspion[ptbins],ptslpion[ptbins],ptslkaon[ptbins],
    ptslproton[ptbins];
59 Float_t etasl[ptbins],etaspion[ptbins],etaslpion[ptbins],etaslkaon[ptbins],
    etaslproton[ptbins];
60 Float_t angles[ptbins],anglespp[ptbins];
61
62
63 Int_t sigmacount = 0, lambdacount = 0, pioncount = 0, daughtercount = 0;
64 Int_t sigmacount2 = 0, lambdacount2 = 0, pioncount2 = 0, daughtercount2 = 0;
65
66
67
68 // Branches
69 t1->Branch("ptspp",&ptspp,"ptspp[8]/F");
70 t1->Branch("ptsppl",&ptsppl,"ptsppl[8]/F");
71 t1->Branch("ptspppion",&ptspppion,"ptspppion[8]/F");
72 t1->Branch("ptspplpion",&ptspplpion,"ptspplpion[8]/F");
73 t1->Branch("ptspplkaon",&ptspplkaon,"ptspplkaon[8]/F");
74 t1->Branch("ptspplproton",&ptspplproton,"ptspplproton[8]/F");
75
76 t1->Branch("etaspp",&etaspp,"etaspp[8]/F");
77 t1->Branch("etasppl",&etasppl,"etasppl[8]/F");
78 t1->Branch("etaspppion",&etaspppion,"etaspppion[8]/F");
79 t1->Branch("etaspplpion",&etaspplpion,"etaspplpion[8]/F");
80 t1->Branch("etaspplkaon",&etaspplkaon,"etaspplkaon[8]/F");
81 t1->Branch("etaspplproton",&etaspplproton,"etaspplproton[8]/F");
82
83 t1->Branch("anglespp",&anglespp,"anglespp[8]/F");
84
85 t1->Branch("nev",&nev,"nev/I");
86 t1->Branch("sigmacount",&sigmacount,"sigmacount/I");
87 t1->Branch("lambdacount",&lambdacount,"lambdacount/I");
88 t1->Branch("pioncount",&pioncount,"pioncount/I");
89 t1->Branch("daughtercount",&daughtercount,"daughtercount/I");
```

```
90
91
92          TFile *f2 = new TFile("50mil_2.root","recreate");
93          TTree *t2 = new TTree("t2","A tree for Sigmac0");
94
95
96  t2->Branch("etas",&etas,"etas[8]/F");
97  t2->Branch("etasl",&etasl,"etasl[8]/F");
98  t2->Branch("etaspion",&etaspion,"etaspion[8]/F");
99  t2->Branch("etaslpion",&etaslpion,"etaslpion[8]/F");
100 t2->Branch("etaslkaon",&etaslkaon,"etaslkaon[8]/F");
101 t2->Branch("etaslproton",&etaslproton,"etaslproton[8]/F");
102
103 t2->Branch("pts",&pts,"pts[8]/F");
104 t2->Branch("ptsl",&ptsl,"ptsl[8]/F");
105 t2->Branch("ptspion",&ptspion,"ptspion[8]/F");
106 t2->Branch("ptslpion",&ptslpion,"ptslpion[8]/F");
107 t2->Branch("ptslkaon",&ptslkaon,"ptslkaon[8]/F");
108 t2->Branch("ptslproton",&ptslproton,"ptslproton[8]/F");
109
110 t2->Branch("sigmacount2",&sigmacount2,"sigmacount2/I");
111 t2->Branch("lambdacount2",&lambdacount2,"lambdacount2/I");
112 t2->Branch("pioncount2",&pioncount2,"pioncount2/I");
113 t2->Branch("daughtercount2",&daughtercount2,"daughtercount2/I");
114
115 t2->Branch("angles",&angles,"angles[8]/F");
116 t2->Branch("nev",&nev,"nev/I");
117
118 // Array of particles
119    TClonesArray* particles = new TClonesArray("TParticle", 1000);
120 // Create pythia8 object
121    TPythia8 *pythia8 = new TPythia8();
122 // Configure
123    pythia8->ReadString("HardQCD:hardccbar = on");
124    pythia8->ReadString("HardQCD:gg2ccbar = on");
125    pythia8->ReadString("HardQCD:qqbar2ccbar = on");
126    pythia8->ReadString("Random:setSeed = 42");
127 //    pythia8->ReadString("Random:seed = 0");
128
129
130 // Initialize
131    pythia8->Initialize(2212 /* p */, 2212 /* p */, 13000. /* TeV */);
132
133 // Event loop
134    for (Int_t iev = 0; iev < nev; iev++) {
135       pythia8->GenerateEvent();
136       if (iev < ndeb) pythia8->EventListing();
137       pythia8->ImportParticles(particles,"All");
138       Int_t np = particles->GetEntriesFast();
139
140
141 // Particle loop
142
143   for (Int_t ip = 0; ip < np; ip++) {
```

```
144
145   TParticle* etacheck = (TParticle*) particles->At(ip);
146   if(TMath::Abs(etacheck->Eta())<0.9) {
147         TParticle* part = (TParticle*) particles->At(ip);
148         Int_t pdg = part->GetPdgCode();
149   // Sigma_C++ decay
150  if(TMath::Abs(pdg) == 4222){
151
152 for(Int_t ipt = 0; ipt < ptbins; ipt++)
153 {
154   if(xmin[ipt]<(part->Pt()) && (part->Pt())<xmax[ipt]){
155
156
157     ptspp[ipt]=part->Pt();
158     etaspp[ipt]=part->Eta();
159
160     sigmacount++;
161     Int_t daughter1 = part->GetFirstDaughter();
162     Int_t daughter2 = part->GetLastDaughter();
163     TParticle* dpart1 = (TParticle*) particles->At(daughter1);
164     TParticle* dpart2 = (TParticle*) particles->At(daughter2);
165     Int_t dpart1pdg = dpart1->GetPdgCode();
166     Int_t dpart2pdg = dpart2->GetPdgCode();
167
168
169     if(TMath::Abs(dpart1pdg) == 4122 || TMath::Abs(dpart2pdg == 4122)){
170       ptsppl[ipt]=dpart1->Pt();
171       etasppl[ipt]=dpart1->Eta();
172       lambdacount++;
173     Int_t ndaughters = dpart1->GetNDaughters();
174     if(ndaughters == 3){
175     Int_t daughterl1 = dpart1->GetFirstDaughter();
176     Int_t daughterl3 = dpart1->GetLastDaughter();
177     TParticle* dlpart1 = (TParticle*) particles->At(daughterl1);
178     TParticle* dlpart2 = (TParticle*) particles->At(daughterl1+1);
179     TParticle* dlpart3 = (TParticle*) particles->At(daughterl3);
180     Int_t dlpart1pdg = dlpart1->GetPdgCode();
181     Int_t dlpart2pdg = dlpart2->GetPdgCode();
182     Int_t dlpart3pdg = dlpart3->GetPdgCode();
183
184     if( ((dlpart1pdg==-321 || dlpart1pdg == 211 || dlpart1pdg == 2212) && (
    dlpart2pdg==-321 || dlpart2pdg == 211 || dlpart2pdg == 2212) && (dlpart3pdg
    ==-321 || dlpart3pdg == 211 || dlpart3pdg == 2212)) ||((dlpart1pdg==321 ||
    dlpart1pdg == -211 || dlpart1pdg == -2212) && (dlpart2pdg==321 ||
    dlpart2pdg == -211 || dlpart2pdg == -2212) && (dlpart3pdg==321 ||
    dlpart3pdg == -211 || dlpart3pdg == -2212))  ){
185     daughtercount++;
186     ptspplkaon[ipt]=dlpart1->Pt();
187     etaspplkaon[ipt]=dlpart1->Eta();
188     ptspplpion[ipt]=dlpart2->Pt();
189     etaspplpion[ipt]=dlpart2->Eta();
190     ptspplproton[ipt]=dlpart3->Pt();
191     etaspplproton[ipt]=dlpart3->Eta();
192     }
```

```
193
194 }
195 }
196     if(TMath::Abs(dpart1pdg) == 211 || TMath::Abs(dpart2pdg) == 211){
197       ptspppion[ipt]=dpart2->Pt();
198       etaspppion[ipt]=dpart2->Eta();
199       pioncount++;
200     }
201
202
203   TVector3 lambdavec(dpart1->Px(),dpart1->Py(),dpart1->Pz());
204     TVector3 pionvec(dpart2->Px(),dpart2->Py(),dpart2->Pz());
205           anglespp[ipt] = TMath::Cos(pionvec.Angle(lambdavec));
206
207 t1->Fill();
208 }
209
210
211   }
212
213   }
214
215
216   // Sigma_C0 decay
217 if((TMath::Abs(pdg) == 4112)){
218
219
220
221 for(Int_t ipt = 0; ipt < ptbins; ipt++)
222 {
223
224   if(xmin[ipt]<(part->Pt()) && (part->Pt())<xmax[ipt]){
225
226
227     pts[ipt]=part->Pt();
228     etas[ipt]=part->Eta();
229
230
231     sigmacount2++;
232     Int_t daughter01 = part->GetFirstDaughter();
233     Int_t daughter02 = part->GetLastDaughter();
234     TParticle* d0part1 = (TParticle*) particles->At(daughter01);
235     TParticle* d0part2 = (TParticle*) particles->At(daughter02);
236     Int_t d0part1pdg = d0part1->GetPdgCode();
237     Int_t d0part2pdg = d0part2->GetPdgCode();
238
239
240     if(TMath::Abs(d0part1pdg) == 4122 || TMath::Abs(d0part2pdg) == 4122){
241       lambdacount2++;
242       ptsl[ipt]=d0part1->Pt();
243       etasl[ipt]=d0part1->Eta();
244     Int_t n0daughters = d0part1->GetNDaughters();
245
246     if(n0daughters == 3){
```

```
247     Int_t daughter0l1 = d0part1->GetFirstDaughter();
248     Int_t daughter0l3 = d0part1->GetLastDaughter();
249     TParticle* d0lpart1 = (TParticle*) particles->At(daughter0l1);
250     TParticle* d0lpart2 = (TParticle*) particles->At(daughter0l1+1);
251     TParticle* d0lpart3 = (TParticle*) particles->At(daughter0l3);
252     Int_t d0lpart1pdg = d0lpart1->GetPdgCode();
253     Int_t d0lpart2pdg = d0lpart2->GetPdgCode();
254     Int_t d0lpart3pdg = d0lpart3->GetPdgCode();
255
256
257     if( ((d0lpart1pdg==-321 || d0lpart1pdg == 211 || d0lpart1pdg == 2212) && (
        d0lpart2pdg==-321 || d0lpart2pdg == 211 || d0lpart2pdg == 2212) && (
        d0lpart3pdg==-321 || d0lpart3pdg == 211 || d0lpart3pdg == 2212)) || ((
        d0lpart1pdg==321 || d0lpart1pdg == -211 || d0lpart1pdg == -2212) && (
        d0lpart2pdg==321 || d0lpart2pdg == -211 || d0lpart2pdg == -2212) && (
        d0lpart3pdg==321 || d0lpart3pdg == -211 || d0lpart3pdg == -2212))){
258     daughtercount2++;
259     ptslkaon[ipt]=d0lpart1->Pt();
260     etaslkaon[ipt]=d0lpart1->Eta();
261     ptslpion[ipt]=d0lpart2->Pt();
262     etaslpion[ipt]=d0lpart2->Eta();
263     ptslproton[ipt]=d0lpart3->Pt();
264     etaslproton[ipt]=d0lpart3->Eta();
265
266     }
267 }
268 }
269     if((d0part1pdg == -211 || d0part2pdg == -211) || (d0part1pdg == 211 ||
        d0part2pdg == 211)){
270       ptspion[ipt]=d0part2->Pt();
271       etaspion[ipt]=d0part2->Eta();
272       pioncount2++;
273       }
274
275     TVector3 lambdavec(d0part1->Px(),d0part1->Py(),d0part1->Pz());
276     TVector3 pionvec(d0part2->Px(),d0part2->Py(),d0part2->Pz());
277           angles[ipt] = TMath::Cos(pionvec.Angle(lambdavec));
278 t2->Fill();
279
280     }
281
282     }
283 }
284
285 }
286   }
287
288 }
289 t1->Print();
290 f1->cd();
291 t1->Write();
292 t2->Print();
293 f2->cd();
294 t2->Write();
```

```
295 printf("there are: \n %i sigmas\n %i lambdas\n %i pions\n %i kaons\n",
        sigmacount,lambdacount,pioncount,daughtercount);
296 printf("and there are: \n %i sigmas\n %i lambdas\n %i pions\n %i kaons\n",
        sigmacount2,lambdacount2,pioncount2,daughtercount2);
297 }
```